AGU PUBLICATIONS

JGR

Journal of Geophysical Research: Biogeosciences

RESEARCH ARTICLE
10.1002/2015JG003283

Key Points:
- Transient flooding events drive large and variable methane emissions from subtropical pastures
- Methane emissions lag water table fluctuations, and peak fluxes occur during water table recession
- Lags are likely driven by surface soil methane dynamics and oxygen pulses delaying emission onset

Supporting Information:
- Supporting Information S1
- Data Set S1
- Data Set S2
- Data Set S3
- Data Set S4

Correspondence to:
S. D. Chamberlain,
sdc84@cornell.edu

Citation:
Chamberlain, S. D., N. Gomez-Casanovas, M. T. Walter, E. H. Boughton, C. J. Bernacchi, E. H. DeLucia, P. M. Groffman, E. W. Keel, and J. P. Sparks (2016), Influence of transient flooding on methane fluxes from subtropical pastures, *J. Geophys. Res. Biogeosci.*, *121*, 965–977, doi:10.1002/2015JG003283.

Received 20 NOV 2015
Accepted 8 MAR 2016
Accepted article online 14 MAR 2016
Published online 29 MAR 2016

©2016. American Geophysical Union. All Rights Reserved.

Influence of transient flooding on methane fluxes from subtropical pastures

Samuel D. Chamberlain[1], Nuria Gomez-Casanovas[2,3,4], M. Todd Walter[5], Elizabeth H. Boughton[6], Carl J. Bernacchi[7], Evan H. DeLucia[2,3,4], Peter M. Groffman[8], Earl W. Keel[6], and Jed P. Sparks[1]

[1]Department of Ecology and Evolutionary Biology, Cornell University, Ithaca, New York, USA, [2]Department of Plant Biology, University of Illinois at Urbana-Champaign, Urbana, Illinois, USA, [3]Energy Biosciences Institute, University of Illinois at Urbana-Champaign, Urbana, Illinois, USA, [4]Institute of Genomic Biology, University of Illinois at Urbana-Champaign, Urbana, Illinois, USA, [5]Department of Biological and Environmental Engineering, Cornell University, Ithaca, New York, USA, [6]MacArthur Agro-ecology Research Center, Lake Placid, Florida, USA, [7]USDA-ARS, Global Change and Photosynthesis Research Unit, Urbana, Illinois, USA, [8]Advanced Science Research Center, City University of New York, New York, New York, USA

Abstract Seasonally flooded subtropical pastures are major methane (CH_4) sources, where transient flooding drives episodic and high-magnitude emissions from the underlying landscape. Understanding the mechanisms that drive these patterns is needed to better understand pasture CH_4 emissions and their response to global change. We investigated belowground CH_4 dynamics in relation to surface fluxes using laboratory water table manipulations and compared these results to field-based eddy covariance measurements to link within-soil CH_4 dynamics to ecosystem fluxes. Ecosystem CH_4 fluxes lag flooding events, and this dynamic was replicated in laboratory experiments. In both cases, peak emissions were observed during water table recession. Flooding of surface organic soils and precipitation driven oxygen pulses best explained the observed time lags. Precipitation oxygen pulses likely delay CH_4 emissions until groundwater dissolved oxygen is consumed, and emissions were temporally linked to CH_4 production in surface soil horizons. Methane accumulating in deep soils did not contribute to surface fluxes and is likely oxidized within the soil profile. Methane production rates in surface organic soils were also orders of magnitude higher than in deep mineral soils, suggesting that over longer flooding regimes CH_4 produced in deep horizons is not a significant component of surface emissions. Our results demonstrate that distinct CH_4 dynamics may be stratified by depth and flooding of surface organic soils drives CH_4 fluxes from subtropical pastures. These results suggest that small changes in pasture water table dynamics can drive large changes in CH_4 emissions if surface soils remain saturated over longer time scales.

1. Introduction

Methane (CH_4) is a globally important greenhouse gas, with a radiative forcing ~25 times higher than CO_2 in the atmosphere, and global CH_4 concentrations have increased 2.5fold since the preindustrial era [*Stocker et al.*, 2013]. Emissions from wetlands and flooded ecosystems are the largest global source of CH_4; however, the magnitudes and controls of these fluxes remain poorly quantified. Much of this uncertainty stems from a poor resolution of flooded area, a lack of measurements across varied wetland ecosystems, and few measurements of the belowground microbial and transport processes mediating surface fluxes [*Riley et al.*, 2011; *Bridgham et al.*, 2013; *Kirschke et al.*, 2013]. Emission estimates are particularly uncertain for seasonally flooded ecosystems where transient flooding drives large and variable CH_4 emissions that are difficult to quantify using traditional in situ chamber measurements [*Melack et al.*, 2004; *Chamberlain et al.*, 2015]. A better understanding of fluxes from these ecosystems is needed to improve our estimates of ecosystem CH_4 emissions and their response to environmental change.

Methane fluxes from flooded ecosystems are the product of CH_4 production, consumption, and transport within soils and water. Here CH_4 is produced exclusively by Archaea (methanogens) that convert end products of fermentation, most notably acetate or CO_2 and H_2, to CH_4 for energy. Methanogens are most active in anaerobic and highly reduced environments, and their activity is generally limited by high oxygen (O_2) concentrations, substrate (C) availability, and the presence of alternative electron acceptors used for respiration [*Conrad*, 2007]. In contrast, CH_4 consuming bacteria (methanotrophs) oxidize CH_4 for energy in the presence of O_2. Methanotrophs are primarily aerobic, and their activity is often limited by low

Table 1. Percent Carbon (C) and Nitrogen (N) Throughout the Pasture Soil Profile ($n = 3$ for All Depths)[a]

Depth (m)	%C	%N
0.0–0.05 (0)	8.48 ± 0.92 *a*	0.49 ± 0.07 *a*
0.05–0.15 (0.1)	3.57 ± 1.58 *a*	0.20 ± 0.10 *b*
0.15–0.25 (0.2)	0.63 ± 0.19 *b*	0.03 ± 0.01 *b*
0.25–0.35 (0.3)	0.20 ± 0.02 *b*	0.09 ± 0.08 *b*
0.35–0.45 (0.4)	0.09 ± 0.01 *b*	0.03 ± 0.02 *b*

[a]Standard errors are reported for all percent C and N values, and letters indicate significant differences between soil horizons for each element (Tukey's honest significant difference (HSD), $P < 0.05$). Depth column indicates the depth range for bulked samples and, in parentheses, the designation used in incubations and mesocosm treatments.

O_2 and CH_4 concentrations [*Conrad*, 2007]. Methanotrophic bacteria are an important moderator of surface emissions and consume significant amounts of soil-produced CH_4 before it reaches the atmosphere [*Oremland and Culbertson*, 1992; *Le Mer and Roger*, 2001; *Teh et al.*, 2006]. Methane production and consumption in soils is often stratified by water table position and oxygen status [*King et al.*, 1990; *Roulet et al.*, 1993; *Conrad et al.*, 1999]; however, both processes can co-occur in well-drained soils that maintain anoxic microsites [*Silver et al.*, 1999; *Teh et al.*, 2005; *Hall et al.*, 2013].

We can better understand the mechanisms controlling ecosystem fluxes by examining flux patterns relative to environmental drivers. In seasonally flooded subtropical pastures, transient flooding produces large and variable CH_4 fluxes that consistently lag flooding events [*Chamberlain et al.*, 2015]. Lagged CH_4 fluxes are commonly observed under fluctuating water table conditions, where maximum fluxes occur during water table recession. In temperate peatlands, it is hypothesized that these patterns are driven by the flooding of a "critical zone" within the soil profile where CH_4 production is maximized (due to favorable redox conditions and substrate availability) or by outgassing of CH_4 produced and stored in deep horizons of the soil profile [*Moore and Dalva*, 1993; *Moore and Roulet*, 1993; *Brown et al.*, 2014]. Subtropical pastures are quite different than temperate peatlands and are characterized by well-drained precipitation-recharged mineral soils. Here oxic conditions may persist below the water table due to large inputs of oxygenated rainwater [*Datry et al.*, 2004; *Schilling and Jacobson*, 2014]. Under these conditions, consumption of oxygen may be incomplete and redox and hydrologic status can become decoupled, allowing anoxic (methanogenesis) and oxic (methanotrophy) processes to co-occur [*Hall et al.*, 2013]. Common observations of flux lags across such contrasting ecosystems suggests that similar mechanisms may drive CH_4 flux dynamics under fluctuating water tables, but these mechanisms have not been evaluated in seasonally flooded subtropical ecosystems.

The goals of this work were to (1) examine patterns in ecosystem CH_4 fluxes under transient flooding events and (2) determine the mechanisms that influence flux time lags. We measured CH_4 fluxes from seasonally flooded subtropical pastures for 3 years using eddy covariance to examine flux patterns relative to hydrologic drivers. To link these ecosystem-scale observations to mechanistic processes, we conducted experimental water table manipulations on intact soil columns to evaluate belowground CH_4 consumption, production, and transport in relation to net surface fluxes. We also conducted an incubation experiment to determine variation in CH_4 production rates throughout the soil profile. These three approaches were used to describe ecosystem flux patterns across transient flooding events and to characterize the mechanistic processes that produce these patterns.

2. Methods

2.1. Study Site

Flux measurements and soils were collected within a fenced improved pasture (92.1 ha) located at the MacArthur Agro-ecology Research Center in Lake Placid, Florida, USA (27.1632004°N, 81.187302°W). The MacArthur Agro-ecology Research Center is a 4290 ha beef cattle ranch that operates as an ecological field station and division of Archbold Biological Station. The pasture is planted with *Paspalum notatum* and is rotationally grazed at a density of ~1.6 cow ha^{-1}. Herbicide and fertilizers have not been applied to the pasture since August 2006 and April 2007, respectively. The pastures receive an average of 1300 mm of rain per year, 75% of which falls during the summer wet season [*Gathumbi et al.*, 2005]. Pastures are developed on Immokalee fine sand spodosols, which are characterized by near-surface organic horizons (0–0.15 m depth) and sandy mineral horizons at depth (0.15–0.50 m depth; Table 1). Within these soils, a spodic horizon is also found at depths greater than 0.5 m below surface. Extensive networks of ditches throughout the pasture

drain these soils, though flooding occurs during heavy rain periods. Mean annual temperature throughout the measurement period was 23.0°C, with a temperature maximum of 35.7°C and minimum of −2.6°C. By area, the study pasture is 74.2% pasture grassland, 10.9% depressional wetland, 9.2% cabbage palm (*Sabal palmetto*) hammock, 4.0% drainage ditch, and 1.7% drainage canal [*Chamberlain et al*., 2015]. All soil samples were collected from pasture grassland, the primary land cover.

2.2. Eddy Covariance and Environmental Measurements

Methane, CO_2, and H_2O fluxes were measured continuously from May 2013 to November 2015 with an eddy covariance tower installed in the pasture center (27.1632004°N, 81.187302°W). Wind speed and direction were measured with a three-dimensional sonic anemometer (CSAT3, Campbell Scientific Inc., Logan, UT), and CH_4, CO_2, and H_2O concentrations were measured with open-path infrared gas analyzers (LI-7700; LI-7500A, Licor Inc., Lincoln, NE). These instruments were installed 2.6 m above the pasture surface and interfaced with a LI-7550 data logger (Licor Inc., Lincoln, NE). Data were collected at 10 Hz and transferred by modem for processing. Water table depth (WTD; meter below surface) was measured at the tower site with a pressure transducer (CS451, Campbell Scientific Inc., Logan, UT), volumetric water content (VWC) was measured at 5, 10, and 20 cm depths with water content reflectometers (CS-616, Campbell Scientific Inc., Logan, UT), and groundwater dissolved oxygen (DO; mg/L) was measured with an optical DO probe installed within the water table well (Aquistar DO2, INW USA, Kent, WA). All auxiliary measures were collected as 30 min averages and logged to a CR3000 data logger (Campbell Scientific Inc., Logan, UT) time synchronized to the LI-7550. Rainfall was measured at 30 min intervals with a tipping bucket gage (TB4, Hydrologic Services America, Lake Worth, FL) at a weather station 1.7 km southwest of the tower (27.150475°N, 81.198568°W). Groundwater DO measurements began in July 2015, and the optical DO probe was installed 0.95 m below the land surface. DO measurements were rejected from analysis if the water table was 0.90 m below surface or deeper. This method has been used in previous studies to continuously monitor groundwater DO concentrations [*Datry et al*., 2004; *Foulquier et al*., 2010; *Schilling and Jacobson*, 2014, 2015].

Methane fluxes were calculated from the covariance of vertical wind speed and CH_4 concentration over 30 min intervals. Raw data were screened for spikes, dropouts, amplitude resolution, absolute value limits, and skewness and kurtosis as described in *Vickers and Mahrt* [1997] and designated default in commercial software (Eddy Pro 4.2, Licor Inc., Lincoln, NE). We used double-rotation tilt corrections to align the anemometer with mean wind streamlines and block averaging to calculate mean wind speed and CH_4 concentration over the 30 min interval. Time lags were corrected with the covariance maximization method. Webb, Pearl, and Leuning corrections for density fluctuations were applied according to *Webb et al*. [1980], and fully analytic spectral corrections were applied according to *Moncrieff et al*. [1997]. All of the above corrections and processing were conducted using commercial software (Eddy Pro 4.2, Licor Inc., Lincoln, NE). We also rejected all fluxes when the open-path CH_4 analyzer was blocked, when CH_4 concentrations were below 1.74 ppm or above 5 ppm, and when fluxes were above 1500 nmol m^{-2} s^{-1} or below −500 nmol m^{-2} s^{-1}, as extreme fluxes and unrealistic concentrations are observed when CH_4 measurement quality is low [*Dengel et al*., 2011; *Baldocchi et al*., 2012].

Data quality were flagged according to *Foken et al*. [2005] using commercial software (Eddy Pro 4.2, Licor Inc., Lincoln, NE). Quality flags range from 1 (best) to 9 (worst). All fluxes with flags greater than 6 were rejected from time series analysis (see section 2.5), and all fluxes with quality flags greater than 3 were rejected when regressing CH_4 fluxes to environmental variables. Overall, 37% of all half-hour fluxes were removed from the time series analysis data set, and 64% of fluxes were removed from the regression analysis data set. For time series analysis, we calculated median daily fluxes and omitted days from analysis with coverage less than 33% as outlined in *Chamberlain et al*. [2015]. Linear regression was used to determine significant relationships between environmental variables and log-transformed daily CH_4 fluxes using only high-quality measured data (quality flags 3 or lower, nongap filled, 33% or higher daily coverage). We calculated daily-integrated fluxes as medians because episodic CH_4 emissions from grazing cattle amplified daily mean fluxes.

2.3. Water Table Manipulations

We conducted laboratory water table manipulations on five intact soil columns. Intact columns were used in this experiment to preserve the pasture soil structure and avoid inaccuracies introduced by slurry-based experiments [*Teh and Silver*, 2006]. Soil columns with live *Paspalum notatum* cover were collected randomly

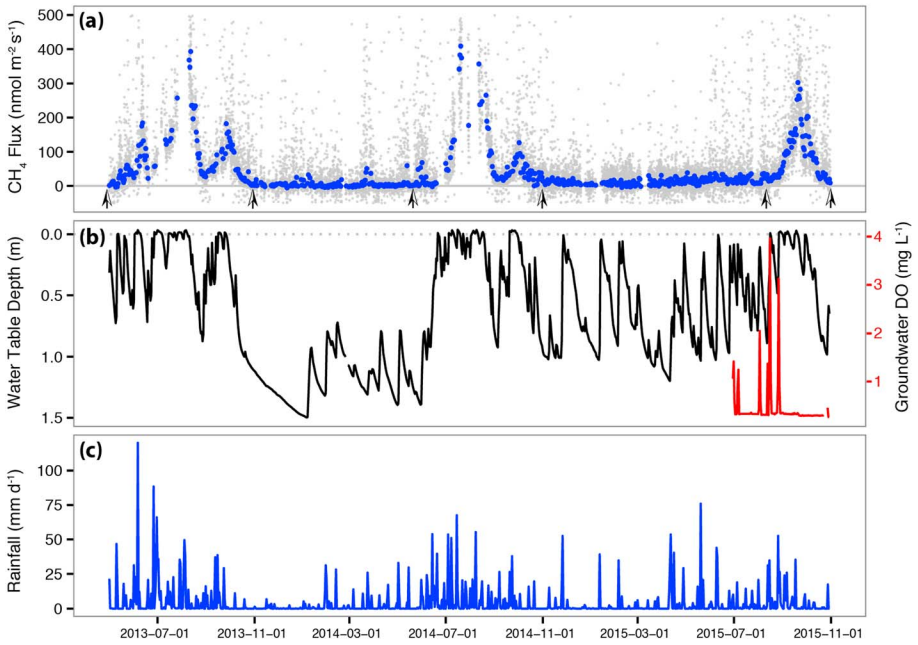

Figure 1. Time series of (a) daily CH_4 fluxes (blue points) and half-hourly CH_4 fluxes (grey points), (b) water table depth and daily mean groundwater DO concentration (red line), and (c) cumulative rainfall. Long periods without flux measurements in July–August 2013 and 2014 correspond to periods of instrument signal dropout. Arrows on Figure 1a mark the beginning and end of flooding periods used in cross-correlation analyses.

in 0.15 × 0.60 m PVC sleeves from pasture within the flux tower footprint in January 2015. PVC sleeves were driven 0.55 m into the ground, and the top 0.05 m was left aboveground to allow surface flux measurements during manipulations. Columns were removed and immediately driven back to Cornell University where water table manipulations were conducted. In all five columns, soil gas and pore water sampling ports were installed at 0, 0.1, 0.2, 0.3, 0.4, and 0.5 m depths with Luer lock fittings. All columns were placed in separate 0.52 × 0.66 m mesocosms, and water was directly added to or removed from the mesocosms to adjust the water table depth. The columns base was left open, allowing water to enter or exit during water table adjustments and equilibrate to the mesocosm water level.

The water table in five replicate mesocosms was increased by 0.1 m increments every 24 h from 0.55 m to 0 m below the surface (seven levels; 0.55, 0.45, 0.35, 0.25, 0.15, 0.05, and 0 m below surface). The water table was left at the surface for 48 h and then decreased at 24 h intervals until mesocosms were dry. The total experiment length was 14 days. While precipitation recharge events in the field are often characterized by sharp jumps in the water table (Figure 1), we chose to simulate a water table recharge and recession event with even tails to fully examine potential hysteresis in the recharge and recession phases. Oxygenated water was introduced to the columns to simulate precipitation recharge groundwater dynamics observed in these pastures (Figure 1). All mesocosms were placed under artificial light (Sunlight Supply, Vancouver, WA) with a 12 h photoperiod, and air temperature was maintained at 22°C.

We measured CH_4 surface fluxes in addition to profile CH_4 concentration and isotopic composition ($\delta^{13}C$-CH_4) in three of five experimental mesocosms (trace gas mesocosms). Only soil gas O_2 and pore water DO were measured in the remaining two mesocosms (oxygen mesocosms). We measured trace gases and oxygen from separate mesocosms to minimize the total volume of soil gas or pore water removed from each column at each time point. By segregating trace gas and oxygen measurements to separate mesocosms, we never evacuated more than 6% of total column soil pore space.

In the trace gas mesocosms, 30 ml of soil gas was removed by syringe from unsaturated soil horizons to measure CH_4 concentrations and $\delta^{13}C$-CH_4. In saturated horizons, 10 ml of pore water was removed by syringe, and dissolved CH_4 was measured by equilibrating pore water with a pure N_2 headspace within the syringe at a 3:1 N_2 to water equilibration ratio [*Jahangir et al.*, 2012]. Equilibrating syringes were placed on an orbital shaker for 10 min and vigorously shaken by hand prior to headspace measurements. All soil and headspace

equilibrated gas samples were analyzed for CH_4 concentration and $\delta^{13}C$-CH_4 on a wavelength-scanned cavity ringdown spectrometer (G2201-*i*, Picarro Inc., Sunnyvale, CA) equipped with a SSIM2 Small Sample Isotope Module (Picarro Inc., Sunnyvale, CA). Gas concentrations in pore water were calculated from headspace concentrations using Henry's law and Bunsen coefficients. Surface fluxes were measured from trace gas mesocosms using a closed dynamic PVC chamber attached to the column surface. The chamber was a closed flow-through design, which circulated the chamber headspace through the spectrometer (G2201-*i*; flow rate 300 ml min^{-1}). When measuring fluxes, the PVC chamber was attached to each column for 5 min, enclosing a 2.55 L volume, and fluxes were calculated by applying a linear regression to concentration increases over the total enclosure period. Concentration and $\delta^{13}C$-CH_4 measurements were precise to within 0.05 ppm CH_4 and 0.8‰. The spectrometer and SSIM2 were calibrated with known concentration and isotope standards of CH_4 in air (Air Liquide, Philadelphia, PA; Isometric Instruments, Victoria, BC). In the two oxygen mesocosms, 30 ml of soil gas was removed from unsaturated horizons by syringe, and soil gas O_2 concentrations were measured with a modified flow-through oxygen sensor (SO-210; Apogee Instruments Inc., Logan, UT). In saturated horizons, 20 ml of pore water was removed and DO was immediately measured using an optical DO sensor (YSI ProDO, Xylem Inc., Rye Brook, NY). Linear regression was used to determine significant relationships between surface CH_4 fluxes and concentration dynamics at different depths within the mesocosms. All mesocosm CH_4 fluxes and concentration measurements were log transformed to meet assumptions of normality.

2.4. Soil Incubations

To compliment the water table manipulations, we also conducted laboratory incubations to assess CH_4 production rates and $\delta^{13}C$-CH_4 of production throughout the soil profile. We removed three intact 0.1×0.55 m cores randomly from the eddy tower footprint in July 2015 following methods described above. In the field, each core was divided into 0–0.5, 0.5–0.15, 0.15–0.25, 0.25–0.35, and 0.35–0.45 m depth sections, homogenized by depth and stored in ziplock bags; these depths correspond to the mesocosm experiment measurement ports (0, 0.1, 0.2, 0.3, and 0.4 depth). Soils were immediately shipped to Cornell University for incubations. Incubation results are reported relative to column measurement ports (0, 0.1, 0.2, 0.3, and 0.4 depth).

For all incubations (15 total), 50 grams of homogenized soil and 100 ml of degassed deionized water were added to 473 ml airtight mason jars fitted with thick butyl rubber stoppers (Geo-Microbial Technologies Inc., Ochleata, OK). All incubation jars were gently swirled by hand to ensure mixing of soil and water. Connection points were further sealed with silicone adhesive. The jar headspace was then purged with 100% N_2 gas for 10 min (flow rate; 500 ml min^{-1}) to create an anaerobic environment. We conducted a 14 day preincubation phase to ensure depletion of O_2 and alternative electron acceptors prior to the measured incubation phase. At the end of preincubation, jars were once again flushed with N_2 for 10 min and measurements began immediately following headspace flushing. Jars were incubated for 21 days in the dark at 22°C, and headspace gases were sampled every 3–4 days. An equivalent volume of 100% N_2 was added when samples were taken to maintain the internal air volume. All gas samples were analyzed for CH_4 concentration and $\delta^{13}C$-CH_4 on the spectrometer (G2201-*i*) equipped with a SSIM2 Small Sample Isotope Module (Picarro Inc., Sunnyvale, CA). An additional jar filled with 10 ppmv CH_4 in air was sampled in tandem with incubations to track potential leakage from jars. No leakage was observed from the 10 ppmv CH_4 jar throughout the 21 day sampling period. After incubations, soils were dried and weighed to allow for calculation of production rates per gram of dry soil (nmol CH_4 g $soil^{-1}$ d^{-1}). Soil CH_4 production rates were then calculated by applying a linear regression to concentration increases across the entire 21 day incubation period (for all regressions; $r^2 > 0.85$; $P < 0.05$). All $\delta^{13}C$-CH_4 data from incubations is presented in supporting information (Figure S1).

We compared mesocosm pore water and anaerobic incubation $\delta^{13}C$-CH_4 values to assess potential fractionation of CH_4 by aerobic oxidation within the mesocosm experiment. The rationale behind this comparison was that aerobic methanotrophic bacteria require oxygen for metabolism [*Conrad*, 2007], and CH_4 produced in anaerobic incubations will not experience aerobic methanotrophic fractionation effects. We also quantified percent carbon (C) and nitrogen (N) for soils collected in the incubation experiment. Homogenized soils were dried for 24 h at 40°C, sieved to 2 mm, and were then analyzed for percent C and N using a LECO C/N analyzer (TruMac, LECO Corporation, St. Joseph, MI).

2.5. Time Series and Diffusive Flux Analysis

We used cross-correlation analyses to quantify the time lag between CH_4 fluxes and water table fluctuations for 184 days for the 2013 and 2014 wet seasons (1 May to 31 October). Cross-correlation analyses were only conducted for wet season periods because the water table did not fluctuate or approach the land surface during other parts of the year. In 2015, cross-correlation analysis was conducted for the active flooding period only (1 August to 31 October). Cross correlations were computed between daily eddy covariance CH_4 fluxes (median; nmol CH_4 m^{-2} s^{-1}) and water table depth. We rejected daily CH_4 fluxes from cross-correlation analysis when less than 33% of CH_4 flux measurements were available. Such periods occurred during July–August of 2013 and 2014 when CH_4 concentration data were not available due to power dropouts and sensor blockage.

We estimated diffusive gas flux rates following *Striegl* [1993] to better understand CH_4 fluxes observed in mesocosms relative to physical properties during water table recession. We estimated diffusive fluxes rates based on three observed mesocosm conditions; when (1) soils were flooded and emissions were low, (2) water tables were recessing and emission peaked, and (3) the water table was lowest, emissions were zero, yet deep horizon CH_4 concentrations were high. Here we estimated diffusive gas fluxes according to the equation:

$$q = -D_{AB}\theta_D\tau\frac{dC_a}{dz}$$

where q = surface flux (nmol m^{-2} d^{-1}), D_{AB} = effective diffusion constant for CH_4 (1.69 m^2 d^{-1} at STP), θ_D = gas-filled porosity, τ = tortuosity, dC_a/dz = CH_4 concentration gradient across depth. τ was assumed to be $\theta_D^{1/3}$ following *Striegl* [1993]. For calculations 1 and 2, we held the concentration gradient constant to quantify the influence of changing gas-filled porosity during water table recession. Here we calculated the gradient using mean atmospheric (0.075 μM CH_4) and 0.1 m depth (0.478 μM) concentrations from days 6 to 9 of the mesocosm experiment. For 3, we calculated q based on the observed concentration gradient on the final day of the mesocosm treatment between the atmosphere (0.075 μM CH_4) and 0.4 m depth (32.85 μM CH_4). θ_D values used in all estimates were calculated as the difference between soil effective porosity and a range of VWC values measured at the eddy tower site during representative pasture conditions (VWC at WTD >= 0 m for scenario 1, 0.15 m > WTD > 0.1 m for scenario 2, and 0.5 m > WTD > 0.4 m for scenario 3). Here effective porosity was assumed to be 0.424, equal to the maximum soil VWC (5 cm depth) measured when pastures were fully flooded. θ_D values used in diffusive flux calculations ranged from 0.000–0.054 for (1), 0.014–0.067 for (2), and 0.020–0.155 for (3). In all calculations, we estimated θ_D from field data because we did not measure VWC in mesocosms. All data processing, analysis, and visualization was conducted in R 3.2.0 using the 'dplyr' and 'ggplot2' packages [*R Core Team*, 2015].

3. Results

Pasture CH_4 emissions were highest during summer wet seasons (Figure 1a), and CH_4 fluxes positively correlated to water table fluctuations ($r^2 = 0.49$, $P < 0.0001$; Figure S2). Transient flooding events were common in these pastures and were characterized by a rapid increase in the water table followed by a more gradual recession following flooding (Figure 1b). Flooding events were most frequent during the wet season and coincided with large and/or frequent precipitation events (Figure 1c). Large and extended ecosystem CH_4 emissions were observed during periods when the water table reached the land surface for more than one day. These events were observed throughout the 2013, 2014, and late 2015 wet seasons (Figure 1). In contrast, appreciable CH_4 emissions were rarely observed during short duration (less than 1 day) or incomplete flooding events that did not reach the land surface. These observations were common from November 2014 to July 2015, when many recharge events occurred, but the water table never reached the land surface for more than a day and no appreciable emissions occurred (Figure 1).

We observed a delay between ecosystem CH_4 fluxes and pasture flooding events, where peak emissions generally occurred during water table recession (Figure 2). This was particularly evident during May–June 2013 when multiple flooding events drove lagged surface fluxes (Figure 2a) and during September–October of 2013, 2014, and 2015 when late season flooding events drove similar lags (Figure 2a—2014 only and Figure 2b—2015 only). These dynamics were observed across year, flooding duration, and emission magnitude (Figure 2). Lags were less evident at the height of the wet season due to periods of sensor dropout when the water table was near the surface for extended periods; however, CH_4 emissions were sustained and

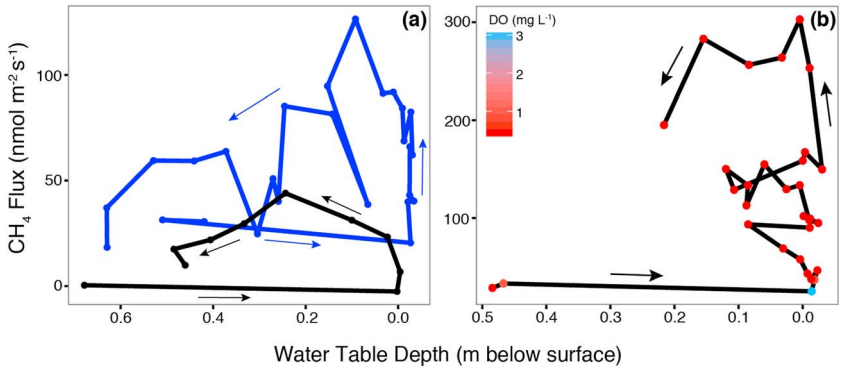

Figure 2. Daily CH_4 fluxes (nmol m^{-2} s^{-1}) across flooding events in (a) 2013 (black line) and 2014 (blue line), and (b) 2015. Events vary in length, year, and emission magnitude. The 2013 event was 9 days (10–19 May 2013), the 2014 event was 26 days (18 September to 14 October 2014), and the 2015 event was 30 days (25 August to September 2015). In 2015, daily mean groundwater dissolved oxygen concentrations (DO; mg L^{-1}) are included as a point heat map. Arrows show directionality of each time series.

lagged the decreasing water table in August of 2013 and 2014 (Figure 1). Correlations between CH_4 fluxes and water table depth were maximized at 3–4 day lags. In 2013, correlations were maximized at a 4 day lag (cross correlation = 0.59; Figure S3), in 2014 at a 3 day lag (cross correlation = 0.56; Figure S3), and in 2015 at a 3 day lag (cross correlation = 0.59; Figure S3). These analyses suggest maximum CH_4 fluxes occur 3–4 days after peak flooding.

Pasture groundwater DO concentrations exhibited pulse dynamics that coincided with periods of pasture flooding and heavy precipitation (Figure 1). During precipitation recharge events that flooded pastures, DO concentrations in groundwater spiked to nearly 30 times background levels (range 0.29–8.08 mg L^{-1}). Following these DO pulses, groundwater DO rapidly reduced to background levels during water table recession (Figures 1 and S4). Connections between CH_4 flux lags and DO were most marked in August 2015 when groundwater DO rapidly increased with flooding (3.96 mg L^{-1}) and then returned to anoxic levels within 1 day ($<$1.0 mg L^{-1}). Here CH_4 emissions were minimized when DO was high and then rapidly increased when DO concentrations decreased (Figure 2b). After the initial flood event, subsequent flooding did not increase groundwater DO concentrations and CH_4 fluxes continued to increase (Figure 2b).

Dissolved oxygen dynamics were reproduced in the mesocosm experiment (Figure 3), and the overall range of DO concentrations in mesocosms were similar to those measured in the field (0.77–7.13 mg L^{-1} in mesocosm; 0.29–8.08 mg L^{-1} in field). Dissolved oxygen concentrations were elevated during water table recharge (days 1–6), rapidly deoxygenated during the flooded phase (days 7–8), and remained reduced during recession (days 9–14; Figure 3). In unsaturated soils, oxygen concentrations were 20.7% (range 19.9–21%) during water table recharge and 19.6% (range 18.5–20.4%) during recession. During recession, soil horizons above the water table adjustment height remained saturated, likely due to capillary action within the soil columns (Figure 3).

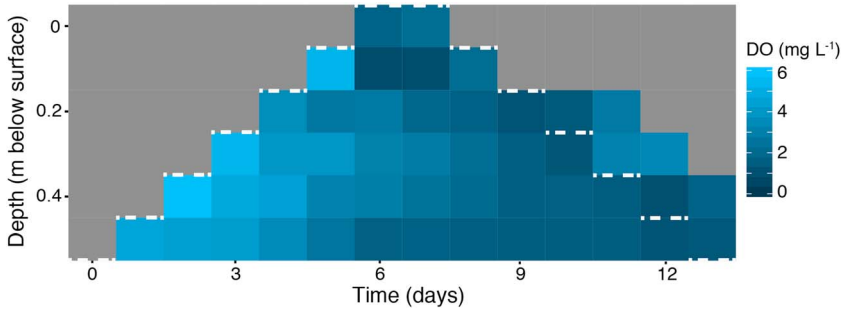

Figure 3. Pore water dissolved oxygen concentrations (DO; mg L^{-1}) throughout water table manipulations. Dissolved oxygen concentrations represent the mean from two replicate mesocosms. The dashed white line represents the location of the water table level outside of the column each day. Grey area represents the unsaturated zone within the soil profile.

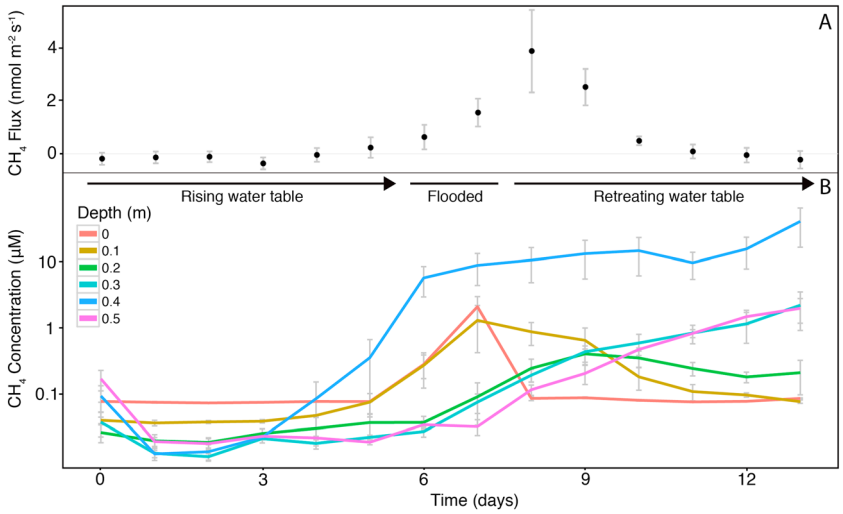

Figure 4. (a) Surface fluxes (nmol CH_4 m^{-2} s^{-1} ± SE) and (b) soil gas and pore water CH_4 concentrations (µM ± SE) throughout mesocosm water table manipulations. During the rising water table, water table depth was increased by 0.1 m per day until the soil surface was flooded, and water levels were reduced by the same interval during the retreating water table.

Lags were reproduced in the mesocosm experiment (Figure 4); however, fluxes in mesocosms were lower than those observed in the field. This difference is likely due to lower levels of C substrate in laboratory water and the relatively short flooding duration (2 days in mesocosm treatments). In mesocosms, near-zero emissions were observed during the recharge phase; emissions began or increased when columns were flooded, peaked, and then tapered back to zero during recession (Figure 4a). Emissions peaked when the water table was 0.05 m below surface during recession (1 day after peak flooding), and fluxes did not return to zero until the water table was 0.35 m below surface, 4 days after peak flooding (Figure 4a). Diffusive flux calculations generally followed these trends; flux estimates were low during flooding (0.00–1.59 nmol CH_4 m^{-2} s^{-1} at 0–0.054 θ_D) and increased as soil gas-filled porosity increased during water table recession (0.26–2.12 nmol CH_4 m^{-2} s^{-1} at 0.014–0.067 θ_D). Diffusive flux calculations also suggest that surface fluxes should be high on the final day of the mesocosm treatment (8.60–131.86 nmol CH_4 m^{-2} s^{-1} at 0.020–0.155 θ_D); however, we observed zero emissions when water tables were lowest and CH_4 concentrations at depth were highest (Figure 4). On the final day, we observed a strong CH_4 concentration gradient from 0.4 m to the surface, and δ^{13}C-CH_4 values enriched toward the surface up to 0.2 m depth. δ^{13}C-CH_4 values at 0.1 m were similar to ambient atmospheric values (Figure 5).

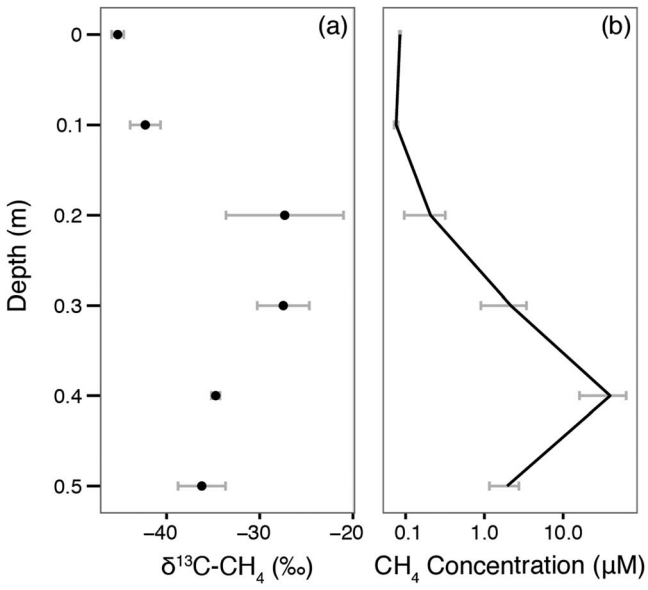

Figure 5. Mean (a) δ^{13}C-CH_4 (‰ ± SD) and (b) CH_4 concentrations (µM ± SE) throughout the soil profile when water table was 0.55 m below surface on the final day of mesocosm manipulations, including both air and pore water measurements. δ^{13}C-CH_4 enrichment from 0.5 to 0.2 m suggests CH_4 oxidation toward the surface.

Distinct CH_4 dynamics were observed between surface organic (0–0.1 m) and deep mineral soils (Table 1 and Figure 4b). Within the surface horizons, CH_4 concentrations increased above ambient at the point of surface flooding then peaked and tapered off over the course of the receding phase (0 and 0.1 m; Figure 4b). Within deep mineral

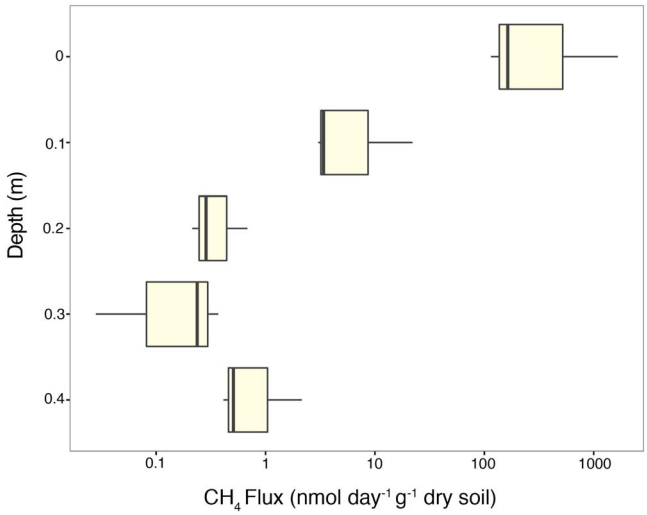

Figure 6. Methane production rates (nmol CH_4 g dry soil^{-1} d^{-1}) by depth in subtropical pasture soils ($n = 3$ per depth). Solid lines are medians, boxes are interquartile ranges (IQR), and whiskers are ± IQR.

horizons, CH_4 concentrations increased above ambient well after initial flooding and continued to rise until complete dry down (0.2–0.5 m depth; Figure 4b). The exception to this was the 0.4 m horizon where elevated concentrations were observed during the recharge phase when the water table was 0.25 m below surface and continued to rise throughout the experiment (Figure 4b). Methane dynamics in surface organic horizons followed emission patterns (Figure 4). Surface fluxes were correlated to CH_4 concentration changes in the 0.1 m horizon ($r^2 = 0.42$; $P < 0.0001$; Figure S5) and poorly correlated to concentration dynamics in all other horizons ($r^2 < 0.18$).

The largest increases in pore water CH_4 concentrations were observed in the 0.4 m horizon, where concentrations were an order of magnitude higher than those observed in any other horizon (Figure 4b). However, this pattern is likely a product of experimental design that caused deeper soils to be flooded for longer durations than surface soils (Figure 3). To isolate the effect of flooded time in the mesocosm experiment, we conducted anaerobic incubations to assess CH_4 production rates of each soil horizon. Anaerobic incubations showed that CH_4 production rates varied by depth (Kruskall-Wallis, $P = 0.02$; Figure 6). Methane production rates were highest in surface organic soils (0–0.05 m; 646.21 ± 507.18 nmol CH_4 g dry soil^{-1} d^{-1}), intermediate in near-surface organic soils (0.05–0.15 m; 9.48 ± 6.27 nmol CH_4 g dry soil^{-1} d^{-1}), and low in deep mineral soils (0.39 ± 0.15, 0.21 ± 0.10, and 1.02 ± 0.56 nmol CH_4 g dry soil^{-1} d^{-1} for horizons 0.15–0.25, 0.25–0.35, and 0.35–0.45 m depth, respectively). Percent C and N data through the soil profile also follow these trends, with the highest percent C and N levels in surface soils (Table 1; Kruskall-Wallis, $P < 0.05$). Percent C content ranged from 8.48 ± 0.92% in surface horizons to 0.09 ± 0.01% in deep horizons (Table 1).

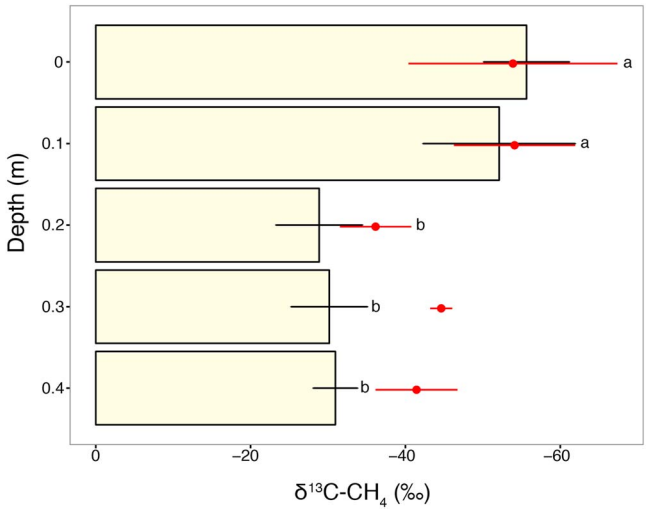

Figure 7. Mean δ^{13}C-CH_4 (‰ ± SD) by depth of pore water samples in mesocosm treatments (bars) and anaerobic incubations (red points, $n = 3$ per depth). Letters denote significant differences between pore water δ^{13}C-CH_4 by depth in mesocosms (Tukey's HSD, $P < 0.05$).

Pore water δ^{13}C-CH_4 values also suggest distinct dynamics between surface and deep soil horizons. δ^{13}C-CH_4 values of pore water varied through the depth profile (analysis of variance, $P < 0.0001$) and were enriched in deep mineral soils relative to surface organic soils (Figure 7). In general, CH_4 isotope values in deep horizons (0.2–0.5 m) varied little during the flooding treatment; however, δ^{13}C-CH_4 in surface soils (0–0.1 m) exhibited higher levels of variability throughout the treatment (Figure S6). Pore water and incubation δ^{13}C-CH_4 were similar in surface organic horizons (Figure 7). In deep horizons, δ^{13}C-CH_4 in anaerobic incubations were somewhat deplete relative to CH_4 observed in pore water, although the range of measured isotope values overlapped in all deep soil horizons (Figure 7).

4. Discussion

In this study, transient precipitation recharge events exerted a major influence on CH_4 emissions from subtropical grassland pastures. Flooding of surface organic soils had the largest influence on emissions, and precipitation recharge DO dynamics appeared to delay the onset of emissions. Complete flooding for 1 day or more was necessary to sustain pasture CH_4 emissions suggesting that surface flooding duration controls the magnitude of emissions. The dynamics described here are potentially relevant to similar ecosystems globally because rainfall is a major driver of inundation in the tropics and subtropics [*Prigent et al*., 2007], and annual emission estimates from these pastures are similar to other flooded ecosystems in these climates [*Chamberlain et al*., 2015]. Generalizability of CH_4 emission estimates is highly desirable for the tropics and subtropics due to a poor representation of flooding and CH_4 dynamics for these regions in global models [*Kirschke et al*., 2013].

We consistently observed peak CH_4 emissions during periods of water table recession (Figure 2). These patterns are well described in temperate peatlands [*Brown et al*., 2014; *Goodrich et al*., 2015] and perhaps suggest common controls to CH_4 fluxes in the two ecosystems. Outgassing of CH_4 stored at depth and flooding of a belowground critical zone of production have both been suggested as potential explanations for observed lags in temperate wetlands [*Moore and Dalva*, 1993; *Moore and Roulet*, 1993; *Brown et al*., 2014]. Our basic diffusive flux modeling suggests that changes in surface soil porosity can induce some outgassing and increased surface emissions, but the gas-filled porosity of surface soils remains low when the water table drops in the field (~1.4–6.7% gas-filled space at 0.05 m depth when WTD 0.1–0.15 m below surface). Based on the small changes we observed in gas-filled porosity during recession, it is unlikely that this factor alone drives emission lags. Additionally, our mesocosm results do not support the hypothesis that the outgassing of CH_4 stored at depth drives lags. Diffusive flux modeling suggests that we should observe the highest fluxes on the final day of the mesocosm experiment when gas-filled pore space (2–16%) and deep CH_4 concentrations are high; however, we observe no surface emission on this day (Figure 4). Instead, it appears that oxidation in upper unsaturated soils may be consuming all deep-produced CH_4 before it reaches the land surface. This can be clearly seen on the final day of the experiment when there is a strong concentration gradient and δ^{13}C-CH_4 enrichment toward the surface (Figure 5). It appears that most of this deep-produced CH_4 is consumed by 0.2 m depth, as δ^{13}C-CH_4 values at 0.1 m are more similar to atmospheric values (Figure 5a). In agreement with temperate observations, our data suggests that flooding of a near-surface organic critical zone is needed for substantial emissions. However, in these subtropical pastures, groundwater DO dynamics appear to control when and if surface fluxes occur.

The influx of oxygenated groundwater to pasture soils likely modulates the onset of fluxes and may explain the observed lags. Here the influx of oxygenated water may delay CH_4 production until groundwater DO is consumed (Figure 2b), and once favorable conditions are in place (i.e., when DO pools are depleted), emissions can be sustained if surface soil horizons remain deoxygenated (Figures 2b, 3, and 4). These affects are most clearly seen in the mesocosm study, where mostly subambient CH_4 concentrations and near-zero emissions were observed during water table recharge with oxygenated groundwater, but emissions and elevated concentrations were observed during recession when groundwater was deoxygenated (Figures 3 and 4). In this example, DO presence likely dampens CH_4 production during water table recharge, though reduced rates of production can still occur in the presence of DO [*Teh et al*., 2005]. Similar DO dynamics relative to emissions were observed over the course of a 2015 flooding event, though we did not observe additional DO influx during subsequent smaller recharge events (Figure 2b). This may result from our probe being unable to capture surface DO influx due to the depth of installation (0.95 m) or from the dilution of oxygenated rainwater into a larger volume of deoxygenated groundwater. Regardless, it appears that DO delays CH_4 emissions during initial groundwater recharge events, though it is unclear whether subsequent rain events dampen CH_4 emissions. Our results do demonstrate that methanogens within these soils respond rapidly to fluctuating redox conditions, in contrast to other wetland systems where CH_4 production lags anoxia from days to weeks [*Cadillo-Quiroz et al*., 2006].

Further research is warranted to better understand the response of microbial communities and CH_4 dynamics to transient DO influx and fluctuating redox conditions, as our work here is primarily observational. However, our work demonstrates that groundwater DO dynamics should be taken into account when assessing greenhouse gas emissions from landscapes experiencing precipitation recharge. Groundwater DO monitoring is

uncommon, and these measurements are generally reported in hydrologic studies that do not account for greenhouse gas fluxes [*Datry et al*., 2004; *Foulquier et al*., 2010; *Schilling and Jacobson*, 2015]. Studies of CH_4 fluxes in precipitation-recharged soils could benefit from additional measurements of groundwater DO. As demonstrated here, these measurements provide an additional mechanism influencing CH_4 emission patterns in ecosystems flooded by wet season rains.

Field and laboratory results both suggest that flooding of surface organic soils influences emission lags. Complete flooding was needed to stimulate emissions from pastures (Figure 1), and peak emissions occurred when the water table retreated through surface horizons (Figure 2). The largest emissions likely occur post-flooding because the water table retreats at a slower rate than it rises, and organic horizons are saturated for longer time periods during recession (Figure 1b). These observations are consistent with laboratory results, where CH_4 dynamics in surface soils exerted the strongest influence on emissions (Figure 4), and CH_4 production rates were orders of magnitude higher in surface soils than in mineral soils below 0.15 m depth (Figure 6). Emissions correlated to CH_4 concentration dynamics in surface soils, while CH_4 in deep mineral soils did not appear to influence emissions (Figure 4). This is particularly apparent on the final day of the mesocosm study, where CH_4 concentrations in deep horizons (0.3–0.5 m) were maximized but surface fluxes were zero (Figure 4). It appears that most of this deep horizon CH_4 is consumed before reaching the surface (Figure 5); however, the orders of magnitude difference in CH_4 production rates between surface organic and deep mineral soil horizons suggests that CH_4 produced at depth is unlikely to be an important component of surface fluxes even if soils are flooded over longer periods (Figure 6).

Large differences in pore water $\delta^{13}C\text{-}CH_4$ values between surface (0–0.1 m) and deep horizons (0.2–0.4 m) further points to distinct CH_4 dynamics stratified through the soil profile. Pore water $\delta^{13}C\text{-}CH_4$ in surface soils was within the range of values expected for biogenic CH_4 production; however, deep horizon values were heavier than expected and outside the accepted range of biogenic CH_4 (Figure 7) [*Whiticar et al*., 1986]. Enriched biogenic $\delta^{13}C\text{-}CH_4$ values are commonly observed when methanotrophs oxidize CH_4; however, studies more commonly observe $\delta^{13}C\text{-}CH_4$ enrichment toward the land surface, as methanotrophs are active in aerobic surface soils [*Liptay et al*., 1998; *Conrad et al*., 1999; *Teh et al*., 2006].

Four mechanisms may explain our observation of unexpectedly high pore water $\delta^{13}C\text{-}CH_4$ values at depth. First, methanotrophs may be active in deep horizons causing CH_4 oxidation and $\delta^{13}C\text{-}CH_4$ enrichment at depth. It is unlikely that aerobic oxidation is responsible for observed fractionation because anaerobic incubation $\delta^{13}C\text{-}CH_4$ values were similar to those observed in mesocosms (Figure 7); however, anaerobic oxidation, which is known to be important in freshwater wetland environments, is also a viable explanation for this observation [*Segarra et al*., 2015]. We do see clear signs of aerobic oxidation on the final day of the mesocosm experiment when soil gas $\delta^{13}C\text{-}CH_4$ enriched in unsaturated horizons toward the surface (Figure 5a).

Second, diffusive fractionation can lead to an enrichment of $\delta^{13}C\text{-}CH_4$ values at depth as $^{12}CH_4$ diffuses through the soil profile more rapidly than $^{13}CH_4$ [*De Visscher et al*., 2004]. This effect likely plays a role in our observations at depth, but $\delta^{13}C\text{-}CH_4$ values measured from our incubation jars were similarly enriched relative to surface soils (Figure 7). Incubation jars were well mixed, and headspace was sampled, minimizing the effect of diffusive fractionation and ruling out diffusion as the sole driver of enrichment at depth within mesocosm pore water.

Third, substrate pool size may influence potential methanogenic fractionation if C substrates are limited in deep mineral horizons. Our results suggest that methanogenic substrates may be limiting in deep horizons, as the C content in these soils was at least 5 times lower than in organic horizons (Table 1), and CH_4 production rates were orders of magnitude lower than organic horizons (Figure 6). The impact of substrate pool limitation on potential fractionation is well described for photosynthetic uptake of CO_2 [*Farquhar and Ehleringer*, 1989], but further incubation studies would be needed to determine if pool effects are driving high $\delta^{13}C\text{-}CH_4$ observations in soil pore water.

Finally, distinct methanogenic communities may be stratified by depth within the soil profile. It is known that the two main functional types of methanogens (acetate fermenting versus CO_2 reducing) fractionate CH_4 to varying degrees [*Chanton et al*., 2004], and methanogenic communities vary across environmental gradients. This community variation is often described through changes in the $\delta^{13}C$ of pore water CH_4 and methanogenic fractionation factors [*Hodgkins et al*., 2014; *Holmes et al*., 2014; *McCalley et al*., 2014]. We observed clear

differences in δ^{13}C-CH_4 between surface and deep soils (Figure 7), which suggests that community composition may vary between organic and mineral soil horizons. In the nearby Everglades, methanogen communities shift across nutrient gradients [*Holmes et al*., 2014], suggesting that similar mechanisms may be important at our site. Further research is needed to determine methanogen community compositions between soil horizons and disentangle these complex isotope effects.

Pasture CH_4 emissions were largely driven by transient flooding of surface organic soils with high CH_4 production rates. This suggests that changes in pasture flooding could cause large changes in net CH_4 emissions if surface organic soils remain saturated over longer time scales. These results are globally significant because pastures are a major land use in subtropical and tropical regions worldwide. Pastures cover 31.4%, 22.7%, and 30.1% of total land area in Central America, tropical South America, and tropical Africa, respectively [*Ramankutty et al*., 2008], so our findings are likely generalizable to areas within these regions that experience wet season flooding. Regionally, pasture is the most common land use in the northern Everglades and covers 35% of total land area [*Hiscock et al*., 2003]. Our results are particularly relevant to the northern Everglades region where water retention practices are implemented to hold floodwater on pastures to reduce nutrient inputs into the downstream Everglades ecosystems [*Bohlen and Villapando*, 2011]. These practices are widely implemented across south Florida [*Bohlen et al*., 2009], and the potential impacts to greenhouse gas emissions have not been assessed. Further research is needed to assess potential emissions resulting from these practices, as our research documents high-magnitude CH_4 emissions from these systems during periods of transient flooding.

Acknowledgments

We thank Hilary Swain, Julia Maki, and the rest of the staff at the MacArthur Agro-ecology Research Center for site access, lodging, transportation, and continued support in the field and thank Suzanne Pierre for help excavating and transporting soil columns. We also thank Mark Conrad for input to analysis and experimental design. This research was supported by Cornell University's Cross-scale Biogeochemistry and Climate Program, Atkinson Center for a Sustainable Future, Department of Ecology and Evolutionary Biology, Andrew W. Mellon Foundation, Cornell Sigma Xi, and University of Illinois USDA ARS. Included in the supporting information are all CH_4 eddy covariance and hydrologic (Table S1), mesocosm CH_4 (Table S2), mesocosm oxygen (Table S3), and incubation (Table S4) data.

References

Baldocchi, D., M. Detto, O. Sonnentag, J. Verfaillie, Y. A. Teh, W. Silver, and N. M. Kelly (2012), The challenges of measuring methane fluxes and concentrations over a peatland pasture, *Agric. For. Meteorol.*, *153*, 177–187.

Bohlen, P. J., and O. R. Villapando (2011), Controlling runoff from subtropical pastures has differential effects on nitrogen and phosphorus loads, *J. Environ. Qual.*, *40*(3), 989–998, doi:10.2134/jeq2010.0127.

Bohlen, P. J., S. Lynch, L. Shabman, M. Clark, S. Shukla, and H. Swain (2009), Paying for environmental services from agricultural lands: An example from the northern Everglades, *Front. Ecol. Environ.*, *7*(1), 46–55, doi:10.1890/080107.

Bridgham, S. D., H. Cadillo-Quiroz, J. K. Keller, and Q. Zhuang (2013), Methane emissions from wetlands: Biogeochemical, microbial, and modeling perspectives from local to global scales, *Global Change Biol.*, *19*(5), 1325–1346, doi:10.1111/gcb.12131.

Brown, M. G., E. R. Humphreys, T. R. Moore, N. T. Roulet, and P. M. Lafleur (2014), Evidence for a nonmonotonic relationship between ecosystem-scale peatland methane emissions and water table depth, *J. Geophys. Res. Biogeosci.*, *119*, 826–835, doi:10.1002/2013JG002576.

Cadillo-Quiroz, H., S. Brauer, E. Yashiro, C. Sun, J. Yavitt, and S. Zinder (2006), Vertical profiles of methanogenesis and methanogens in two contrasting acidic peatlands in central New York State, USA, *Environ. Microbiol.*, 1428–1440.

Chamberlain, S. D., E. H. Boughton, and J. P. Sparks (2015), Underlying ecosystem emissions exceed cattle-emitted methane from subtropical lowland pastures, *Ecosystems*, *8*(6), 933–945, doi:10.1007/s10021-015-9873-x.

Chanton, J., L. Chaser, and P. Glasser (2004), Carbon and hydrogen isotopic effects in microbial methane from terrestrial environments, in *Stable Isotopes and Biosphere-atmosphere Interactions*, pp. 85–105, Elsevier, Atlanta, Ga.

Conrad, M. E., A. S. Templeton, P. F. Daley, and L. Alvarez-Cohen (1999), Seasonally-induced fluctuations in microbial production and consumption of methane during bioremediation of aged subsurface refinery contamination, *Environ. Sci. Technol.*, *33*(22), 4061–4068, doi:10.1021/es990582o.

Conrad, R. (2007), Microbial ecology of methanogens and methanotrophs, in *Advances in Agronomy*, vol. 96, pp. 1–63, Elsevier, Atlanta, Ga.

Datry, T., F. Malard, and J. Gibert (2004), Dynamics of solutes and dissolved oxygen in shallow urban groundwater below a stormwater infiltration basin, *Sci. Total Environ.*, *329*(1–3), 215–229, doi:10.1016/j.scitotenv.2004.02.022.

De Visscher, A., I. De Pourcq, and J. Chanton (2004), Isotope fractionation effects by diffusion and methane oxidation in landfill cover soils, *J. Geophys. Res.*, *109*, D18111, doi:10.1029/2004JD004857.

Dengel, S., P. E. Levy, J. Grace, S. K. Jones, and U. M. Skiba (2011), Methane emissions from sheep pasture, measured with an open-path eddy covariance system, *Global Change Biol.*, *17*(12), 3524–3533, doi:10.1111/j.1365-2486.2011.02466.x.

Farquhar, G. D., and J. R. Ehleringer (1989), Carbon isotope discrimination and photosynthesis, *Annu. Rev. Plant Physiol. Plant Mol. Biol*, *40*, 503–537.

Foken, T., M. Göockede, M. Mauder, L. Mahrt, B. Amiro, and W. Munger (2005), Post-field data quality control, in *Handbook of Micrometeorology*, edited by X. Lee, W. J. Massman, and B. E. Law, pp. 181–208, Kluwer Acad., Dordrecht, Netherlands.

Foulquier, A., F. Malard, F. Mermillod-Blondin, and T. Datry (2010), Vertical change in dissolved organic carbon and oxygen at the water table region of an aquifer recharged with stormwater: Biological uptake or mixing? *Biogeochemistry*, *99*(1–3), 31–47, doi:10.1007/s10533-009-9388-7.

Gathumbi, S. M., P. J. Bohlen, and D. A. Graetz (2005), Nutrient enrichment of wetland vegetation and sediments in subtropical pastures, *Soil Sci. Soc. Am. J.*, *69*(2), 539–548.

Goodrich, J. P., D. I. Campbell, and N. T. Roulet (2015), Overriding control of methane flux temporal variability by water table dynamics in a Southern Hemisphere, raised bog, *J. Geophys. Res. Biogeosci.*, 819–831, doi:10.1002/2014JG002844.

Hall, S. J., W. H. McDowell, and W. L. Silver (2013), When wet gets wetter: Decoupling of moisture, redox biogeochemistry, and greenhouse gas fluxes in a humid tropical forest soil, *Ecosystems*, *16*(4), 576–589, doi:10.1007/s10021-012-9631-2.

Hiscock, J. G., C. S. Thourot, and J. Zhang (2003), Phosphorus budget-land use relationships for the northern Lake Okeechobee watershed, Florida, *Ecol. Eng.*, *21*, 63–74, doi:10.1016/j.ecoleng.2003.09.005.

Hodgkins, S. B., M. M. Tfaily, C. K. McCalley, T. A. Logan, P. M. Crill, S. R. Saleska, V. I. Rich, and J. P. Chanton (2014), Changes in peat chemistry associated with permafrost thaw increase greenhouse gas production, *Proc. Natl. Acad. Sci. U.S.A.*, *111*(16), 5819–5824, doi:10.1073/pnas.1314641111.

Holmes, M. E., J. P. Chanton, and H. S. Bae (2014), Effect of nutrient enrichment on $\delta^{13}CH_4$ and the methane production pathway in the Florida Everglades, *J. Geophys. Res. Biogeosci.*, *119*, 1267–1280, doi:10.1002/jgrg.20122.

Jahangir, M. M. R., P. Johnston, M. I. Khalil, J. Grant, C. Somers, and K. G. Richards (2012), Evaluation of headspace equilibration methods for quantifying greenhouse gases in groundwater, *J. Environ. Manage.*, *111*, 208–212, doi:10.1016/j.jenvman.2012.06.033.

King, G. M., P. Roslev, and H. Skovgaard (1990), Distribution and rate of methane oxidation in sediments of the Florida Everglades, *Appl. Environ. Microbiol.*, *56*(9), 2902–2911.

Kirschke, S., P. Bousquet, P. Ciais, M. Saunois, J. G. Canadell, E. J. Dlugokencky, P. Bergamaschi, D. Bergmann, D. R. Blake, and L. Bruhwiler (2013), Three decades of global methane sources and sinks, *Nat. Geosci.*, *6*(10), 813–823, doi:10.1038/ngeo1955.

Le Mer, J., and P. Roger (2001), Production, oxidation, emission and consumption of methane by soils: A review, *Eur. J. Soil Biol.*, *37*(1), 25–50.

Liptay, K., J. Chanton, P. Czepiel, and B. Mosher (1998), Use of stable isotopes to determine methane oxidation in landfill cover soils, *J. Geophys. Res.*, *103*(D7), 8243–8250, dzoi:10.1029/97JD02630.

McCalley, C. K., et al. (2014), Methane dynamics regulated by microbial community response to permafrost thaw, *Nature*, *514*(7523), 478–481, doi:10.1038/nature13798.

Melack, J. M., L. L. Hess, M. Gastil, B. R. Forsberg, S. K. Hamilton, I. B. Lima, and E. M. Novo (2004), Regionalization of methane emissions in the Amazon Basin with microwave remote sensing, *Global Change Biol.*, *10*(5), 530–544, doi:10.1111/j.1529-8817.2003.00763.x.

Moncrieff, J. B., J. M. Massheder, H. De Bruin, J. Elbers, T. Friborg, B. Heusinkveld, P. Kabat, S. Scott, H. Søgaard, and A. Verhoef (1997), A system to measure surface fluxes of momentum, sensible heat, water vapour and carbon dioxide, *J. Hydrol.*, *188*, 589–611.

Moore, T. R., and M. Dalva (1993), The influence of temperature and water table position on carbon dioxide and methane emissions from laboratory columns of peatland soils, *J. Soil Sci.*, *44*(4), 651–664.

Moore, T. R., and N. T. Roulet (1993), Methane flux: Water table relations in northern wetlands, *Geophys. Res. Lett.*, *20*(7), 587–590, doi:10.1029/93GL00208.

Oremland, R. S., and C. W. Culbertson (1992), Importance of methane-oxidizing bacteria in the methane budget as revealed by the use of a specific inhibitor, *Nature*, *356*(6368), 421–423.

Prigent, C., F. Papa, F. Aires, and W. B. Rossow (2007), Global inundation dynamics inferred from multiple satellite observations, 1993–2000, *J. Geophys. Res.*, *112*, D12107, doi:10.1029/2006JD007847.

R Core Team (2015), *R: A Language and Environment for Statistical Computing*, R Foundation for Statistical Computing, Vienna, Austria. [Available at http://www.R-project.org/.]

Ramankutty, N., A. T. Evan, C. Monfreda, and J. A. Foley (2008), Farming the planet: 1. Geographic distribution of global agricultural lands in the year 2000, *Global Biogeochem. Cycles*, *22*, GB1003, doi:10.1029/2007GB002952.

Riley, W. J., Z. M. Subin, D. M. Lawrence, S. C. Swenson, M. S. Torn, L. Meng, N. M. Mahowald, and P. Hess (2011), Barriers to predicting changes in global terrestrial methane fluxes: Analyses using CLM4Me, a methane biogeochemistry model integrated in CESM, *Biogeosci. Discuss.*, *8*(1), 1733–1807, doi:10.5194/bg-8-1925-2011.

Roulet, N. T., R. Ash, W. Quinton, and T. Moore (1993), Methane flux from drained northern peatlands: Effect of a persistent water table lowering on flux, *Global Biogeochem. Cycles*, *7*(4), 749–769, doi:10.1029/93GB01931.

Schilling, K. E., and P. J. Jacobson (2014), Temporal variations in dissolved oxygen concentrations observed in a shallow floodplain aquifer, *River Res. Appl.*, doi:10.1002/rra.2759.

Schilling, K. E., and P. Jacobson (2015), Field observation of diurnal dissolved oxygen fluctuations in shallow groundwater, *Ground Water*, *53*(3), 493–497, doi:10.1111/gwat.12218.

Segarra, K. E. A., F. Schubotz, V. Samarkin, M. Y. Yoshinaga, K.-U. Hinrichs, and S. B. Joye (2015), High rates of anaerobic methane oxidation in freshwater wetlands reduce potential atmospheric methane emissions, *Nat. Commun.*, *6*, 7477, doi:10.1038/ncomms8477.

Silver, W. L., A. E. Lugo, and M. Keller (1999), Soil oxygen availability and biogeochemistry along rainfall and topographic gradients in upland wet tropical forest soils, *Biogeochemistry*, *44*(3), 301–328, doi:10.1023/A:1006034126698.

Stocker, T. F., et al. (2013), Technical Summary, in *Climate Change 2013: The Physical Science Basis. Contribution of Working Group I to the Fifth Assessment Report of the Intergovernmental Panel on Climate Change*, edited by T. F. Stocker et al., Cambridge Univ. Press, New York.

Striegl, R. G. (1993), Diffusional limits to the consumption of atmospheric methane by soils, *Chemosphere*, *26*(1–4), 715–720.

Teh, Y. A., and W. L. Silver (2006), Effects of soil structure destruction on methane production and carbon partitioning between methanogenic pathways in tropical rain forest soils, *J. Geophys. Res.*, *11*, G01003, doi:10.1029/2005JG000020.

Teh, Y. A., W. L. Silver, and M. E. Conrad (2005), Oxygen effects on methane production and oxidation in humid tropical forest soils, *Global Change Biol.*, *11*, 1283–1297, doi:10.1111/j.1365-2486.2005.00983.x.

Teh, Y. A., W. L. Silver, M. E. Conrad, S. E. Borglin, and C. M. Carlson (2006), Carbon isotope fractionation by methane-oxidizing bacteria in tropical rain forest soils, *J. Geophys. Res.*, *111*, G02001, doi:10.1029/2005JG000053.

Vickers, D., and L. Mahrt (1997), Quality control and flux sampling problems for tower and aircraft data, *J. Atmos. Oceanic Technol.*, *14*(3), 512–526.

Webb, E. K., G. I. Pearman, and R. Leuning (1980), Correction of flux measurements for density effects due to heat and water vapour transfer, *Q. J. R. Meteorol. Soc.*, *106*(447), 85–100.

Whiticar, M. J., E. Faber, and M. Schoell (1986), Biogenic methane formation in marine and freshwater environments: CO_2 reduction vs. acetate fermentation—Isotope evidence, *Geochim. Cosmochim. Acta*, 693–709.